Presented to "ONR Workshop on Free-Electron Lasers" - Sun Valley, June 22-25, 1981

ISTITUTO NAZIONALE DI FISICA NUCLEARE
Laboratori Nazionali di Frascati

LNF-81/44(P)
14 Luglio 1981

R. Barbini and G. Vignola:

FEL PROGRAM AT THE ADONE STORAGE RING.

Servizio Documentazione
dei Laboratori Nazionali di Frascati
Cas. Postale 13 - Frascati (Roma)

INFN - Laboratori Nazionali di Frascati
Servizio Documentazione

LNF-81/44(P)
14 Luglio 1981

R. Barbini and G. Vignola:

FEL PROGRAM AT THE ADONE STORAGE RING.

Presented to:

"ONR Workshop on Free-Electron Lasers"
Sun Valley, Idaho, June 22-25, 1981

FEL PROGRAM AT THE ADONE STORAGE RING[+]

R. Barbini[x] and G. Vignola[x]

INFN - Laboratori Nazionali di Frascati
Frascati, Italy

1. INTRODUCTION

In the last few years there has been an increasing on the study of free electron lasers. The experiments performed by Madey and coworkers with the Stanford Superconducting Linac showed that it is possible to achieve both amplification[1] of the coherent radiation and laser oscillation[2] by sending an electron beam through the periodic field of a magnetic undulator.

More recently, a successful amplification experiment has been carried out at the ACO storage ring[3], in the visible region (4880-5145 Å), where a maximum peak gain of 5.6×10^{-4}/pass was measured.

[+] This activity is performed in the framework of a collaboration among the INFN-LNF Accelerator and Technical Divisions and the University of Naples.

[x] On leave from CNEN - Centro di Frascati.

Tunability over a wide wavelength range (0.1-20 μm), reasonably sharp linewidth ($\Delta\lambda/\lambda = 10^{-7} \div 10^{-4}$) and the promise of high output power and efficiency make this type of laser an attractive tool for research in many fields such as photochemistry, molecular physics, solid state physics, etc.

If by the aid of technical improvements the average output power will reach the predicted kW level with efficiency of some percent, many industrial applications and probably laser isotope separation could benefit from this new kind of laser.

Various theoretical approaches have been attempted and many models introduced for explaining the (scarce) experimental data and for anticipating the FEL interaction features, also in connection with the possible electron accelerator to be used (linacs, storage rings, etc.). However, we believe the interaction between radiation and the recirculated e-beam of a storage ring to be still worth of accurate investigation, and we therefore designed a feasibility FEL experiment (LELA)[4] to be mounted in Adone, in order to collect information on:

- amplification of radiation with the aid of an external Argon laser ($\lambda = 5145$ Å);
- wavelength and optical gain as functions of electron energy and undulator magnetic field;
- transient behaviour of the laser radiation;
- steady-state interaction between laser radiation and stored electrons (i.e. optical gain vs. electron energy, maximum extractable optical power, optical spectrum, elec

tron bunch lengthening and energy heating, etc.).

An experimental check of the gain for higher harmonics and for an optical klystron configuration is also planned.

A successful LELA operation will place on a solid experimental ground the performance of an existing storage ring in connection with the FEL interaction, and, moreover, will provide essential information for a possible FEL dedicated storage ring.

2. THE SPONTANEOUS RADIATION FROM A TRANSVERSE UNDULATOR.

The characteristics of radiation emitted by an electron beam in passing through a magnetic field have a well refined theoretical treatment and extensive review papers have been written on this argument[5].

Nevertheless care must be taken in using the radiation formulae developed for simple bending magnets when dealing with multipole magnets such as undulators : in this case a proper summation must be accomplished of the various poles contributions to the overall radiation which accounts for the appearence of a line structure in the radiation spectra.

We just summarize here the principal results in connection with the FEL physics.

By defining for a plane undulator with period λ_q the adimensional strength parameter K as

$$K = \frac{eB_{RMS}\lambda_q}{2\pi m c^2} \simeq 9.3\, B_{RMS}\,(KG)\,\lambda_q(m) \qquad (1)$$

where B_{RMS} is the RMS vertical magnetic field on axis:

$$B_{RMS} = \left[\frac{1}{\lambda_q}\int_0^{\lambda_q} B_z(y)^2\,dy\right]^{1/2}, \qquad (2)$$

the spontaneous radiation energy emitted on the undulator axis by an electron with energy $\gamma = E/mc^2$ is made up of harmonics centered around the wavelengths

$$\lambda_h = \frac{1}{h}\frac{\lambda_q}{2\gamma^2}(1 + K^2) \qquad (h = 1, 3, 5, \ldots). \qquad (3)$$

The distribution is well represented by the $\mathrm{sinc}^2 x_\lambda$ function with $x_\lambda = N\pi h(\lambda - \lambda_h)/\lambda$, N being the total number of undulator periods, and has a percent FWHM

$$\frac{\Delta\lambda}{\lambda_h} \simeq \frac{1}{hN}. \qquad (4)$$

The first harmonic (h = 1) distribution peak value can be expressed as

$$\left.\frac{d^2I}{d\omega\,d\Omega}\right|_{\substack{\vartheta = 0\\ \lambda = \lambda_1}} \simeq 9.6 \times 10^{-24} F(K) \left(\frac{NK\gamma}{1+K^2}\right)^2 \qquad (5)$$

(MeV · sec/sr).

The function F(K) arises from the flat simmetry of the undulator. As a matter of fact, in a plane undulator the electron velocity oscillates also along the longitudinal coordinate (with a period $\lambda_q/2$). Insertion of the exact longitudinal velocity (in place of its average value) in the Liénard Wiechert

radiation formula[6] results in a slight decrease of the energy emitted per unit solid angle and bandwidth, which turns out to depend only upon the undulator strength parameter K. This feature has been numerically checked by our radiation code SINCLUCE[7], which provided for F(K) the curve shown in Fig. 1.

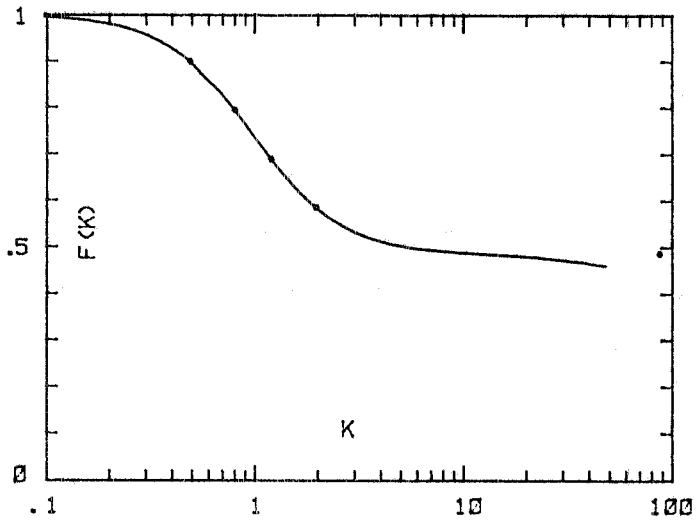

Fig. 1. The function F(K). The solid curve is computed by SINCLUCE. Dots corresponds to eq. (6) for some K values.

The same effect will be reflected on the gain expression, as first pointed out in Ref. 8, where the analytic expression of F(K) has been worked out, in terms of the Bessel functions J_o, J_1:

$$F(K) = \left[J_o(\xi) - J_1(\xi) \right]^2 \qquad (6)$$

with

$$\xi = \frac{K^2/2}{1 + K^2} \quad .$$

According to the terminology of Ref. 9, the peak intensity envelope for the various harmonics is described by the function

$$N_2(\varepsilon_h, 0) = \frac{1}{\varepsilon_h^2} K_{2/3}^2 \left(\frac{1}{2\varepsilon_h}\right) \tag{7}$$

ε_h being the normalized wavelength

$$\varepsilon_h = \frac{\lambda_h}{\lambda_c} = \frac{3\sqrt{2}}{4} \frac{1}{h} K(1 + K^2) \tag{8}$$

and $K_{2/3}$ the modified Bessel function of order 2/3.

As shown in Fig. 2, higher harmonics can have a peak intensity either higher or lower than the first, depending only on the K value: the pivot point occurs at $\varepsilon_h \simeq 1.25$, corresponding to $K \simeq 0.75$.

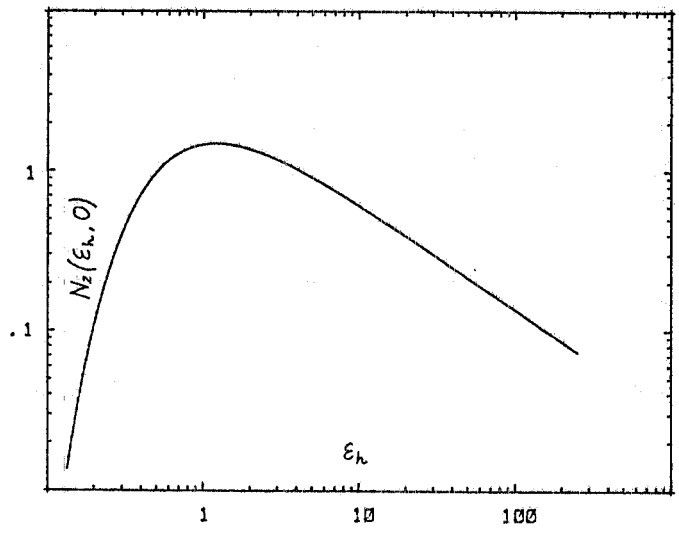

Fig. 2. Envelope of the radiation peak intensity vs. normalized wavelength. The curve can be used for obtaining the higher harmonics peak intensity relative to the first one.

3. THE FEL GAIN

Provided the e-beam bunch is fully contained within the transverse photon bunch dimensions (averaged mode section = $\langle \Sigma_L \rangle$), the FEL small signal gain per pass in the homogeneous broadening regime and for a monochromatic e-beam reads[10]:

$$g_o = -32\sqrt{2}\pi^2 \lambda^{3/2} \lambda_q^{1/2} \frac{K^2}{(1+K^2)^{3/2}} \cdot \frac{I_p}{I_A} \frac{N^3}{\langle \Sigma_L \rangle} f(x_\gamma) \cdot F(K) \tag{9}$$

where

$$I_A = \frac{ec}{r_o} = 17000 \text{ A},$$

I_p = peak current/bunch,

$$x_\gamma = 4\pi N \frac{\gamma_o - \gamma_R}{\gamma_R},$$

γ_o = working energy (in unit of mc^2),

$$\gamma_R = \text{resonance energy} = \left[\frac{\lambda_q}{2}(1+K^2)\right]^{1/2},$$

$$f(x_\gamma) = \frac{1}{x_\gamma^3}\left[\cos x_\gamma - 1 + \frac{1}{2} x_\gamma \sin x_\gamma\right].$$

The function $f(x_\gamma)$ is plotted in Fig. 3 and is proportional to the derivative with respect to x_γ (i.e. electron energy) of the on axis spontaneous emission lineshape ($\sin c^2 x_\gamma/2$) homogeneously broadened.

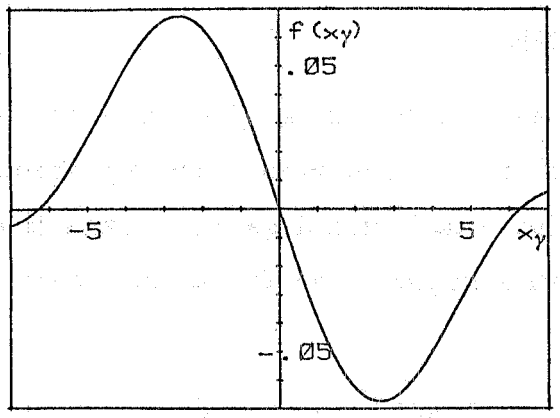

Fig. 3. The gain profile.

This relationship between spontaneous radiation and gain is a general result[11] which we consider to be applicable to our experimental configuration (i. e. e-beam quality and undulator symmetry) and which will again be used (see below).

4. THE UNDULATOR

Simplicity and flexibility have been the basic criteria in choosing the LELA-experiment parameters. Unnecessary technical complications are avoided by operating in the visible wavelength region and by adopting standard electromagnet technology. The electron energy should be the highest possible in order to store the maximum peak current in the ring. The undulator period has been designed so as to accomodate the maximum number of periods in the fixed length (2.5 m) of the Adone straight section. Finally, electron energy, undulator period and magnetic field must satisfy the wavelength equation (3).

According to the above considerations the basic LELA

parameters have been chosen as follows: energy $E \simeq 600$ MeV, radiation wavelength $\lambda \simeq 5000$ Å, $K \simeq 3.4$.

The undulator is shown in Figs. 4, 5, and its characteristics are listed in Table I.

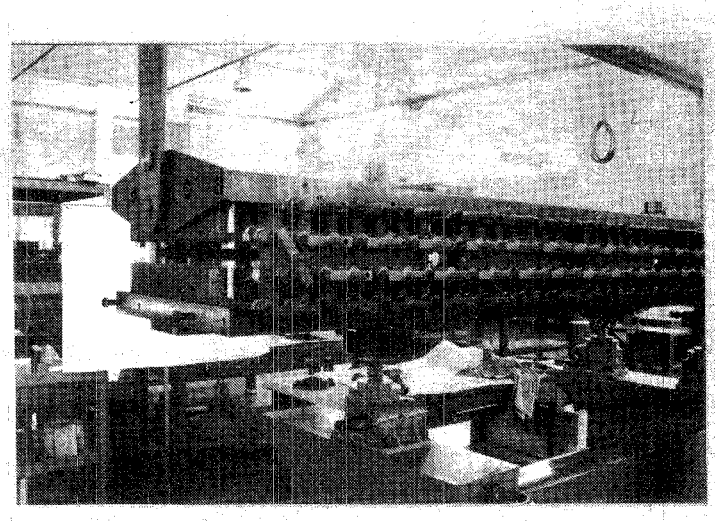

Fig. 4. Overall view of the assembled undulator.

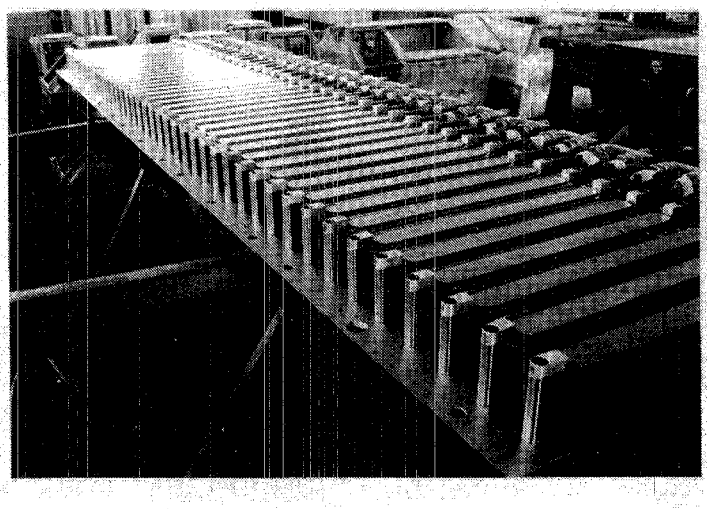

Fig. 5. Lower half of the undulator, showing pole pieces, coils and electrical-hydraulic connections.

Table I - Undulator characteristics.

Undulator period	11.6 cm
Number of poles	39 full poles + 2 half poles
Total length (with clamps)	2.412 m
Gap height	4.0 cm
Pole length	2.9 cm
Pole height.....	6.5 cm
Pole width	34.8 cm
Core weight	1800 Kg
Copper weight	287 KG
Design current	3150 A
Current density	30 A/mm^2
Total power dissipation @ 3150 A	550 KW
Peak vertical field on axis	4.95 KG

The vertical field on the median plane as computed by the MAGNET code[12], and measured on a double wavelength full scale prototype[13] is plotted in Figs. 6, 7 for an inner pole and for the end pole plus the clamping plate, respectively.

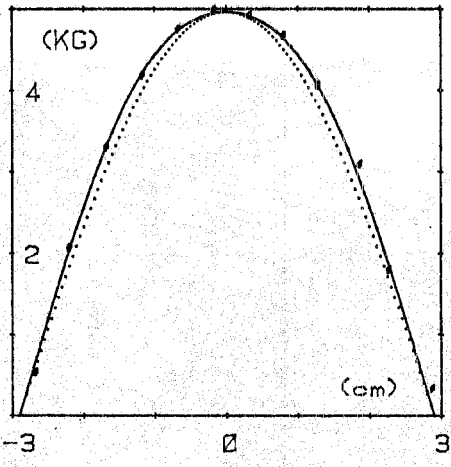

Fig. 6. Vertical field on axis vs. the longitudinal coordinate, under an inner pole. Solid curve is computed by MAGNET. Dots are measured values. Dotted curve is a "cos-like" normalized to the maximum field.

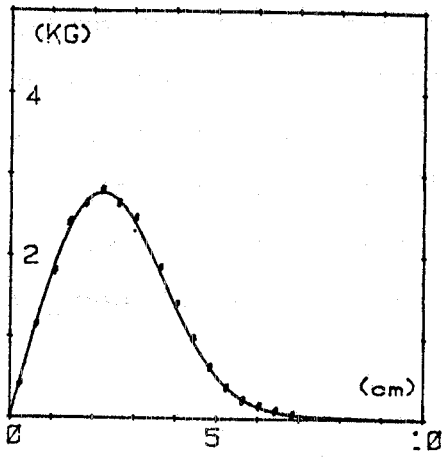

Fig. 7. Vertical field on axis vs. the longitudinal coordinate, under an end pole plus clamping plate. Solid curve is computed by MAGNET. Dots are measured values.

Finally, on Fig. 8 the strength K as defined in eq. (1) and measured on the undulator prototype is shown.

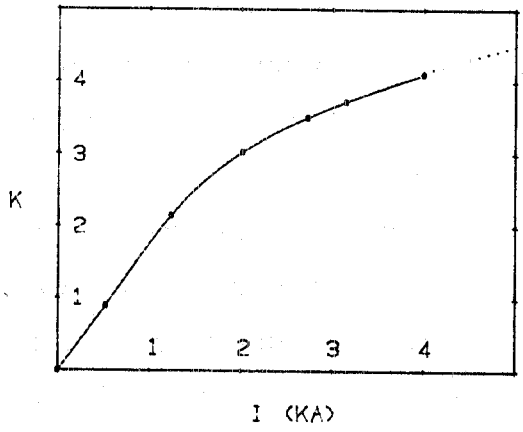

Fig. 8. The undulator strength K versus current in the coils.

By extrapolating this measurement to the final undulator, we can safely assume that a value of K=4 will be easily exceeded.

The undulator is to be installed in the Adone straight sec

tion no. 11 as shown in Fig. 9, where the experiment layout is schematically sketched. We remark that a vanishing field integral along the longitudinal coordinate must be achieved, insofar as the undulator is to be mounted in a storage ring. This goal will be reached statically by machining the end poles to the correct length and by clamping the field width additional plates.

5. STORAGE RING OPTICS

We require the e-beam transverse dimension to be a minimum at the FEL interaction region.

By recalling[14] that the total radial spread can be written as

$$\sigma_x^2 = \sigma_{x\beta}^2 + \sigma_{x\varepsilon}^2 \qquad (10)$$

we can cancel out the synchrotron contribution $\sigma_{x\varepsilon}$ by imposing the off energy η function to be vanishing at the location where the undulator will be mounted[4].

By increasing the number of independent quadrupole families from 2 to 4, Adone can be made into a six-period machine with η vanishing in alternate straights. The resulting optical functions are plotted in Figs. 10 and 11 for the radial and vertical plane, respectively.

From the standpoint of machine optics, the undulator acts as a vertical focussing quadrupole[4, 15], so that vertical betatron function β_z must be slightly changed, in order to preserve matching when the undulator is switched on. This is shown in Fig. 11. The Adone parameters resulting from the

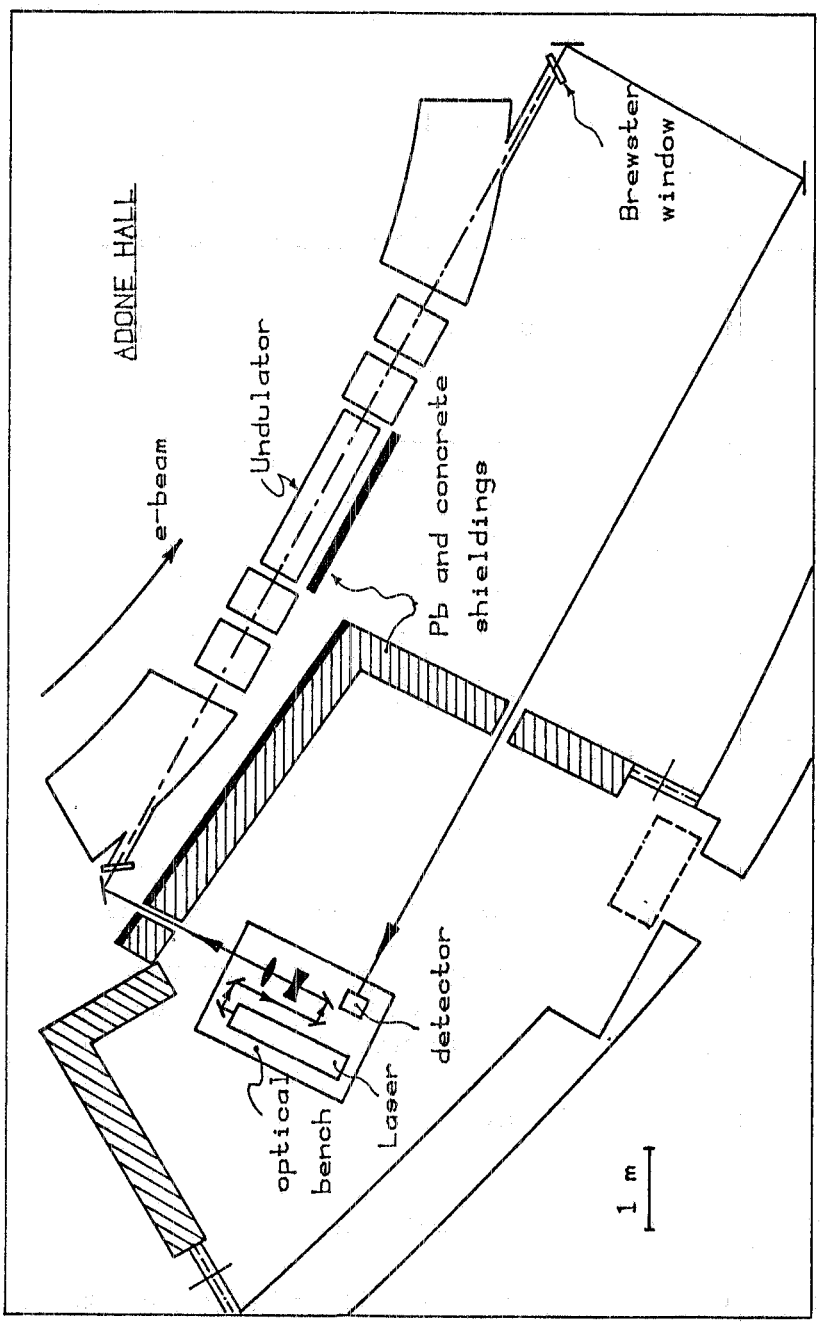

Fig. 9. Layout of the LELA experimental area.

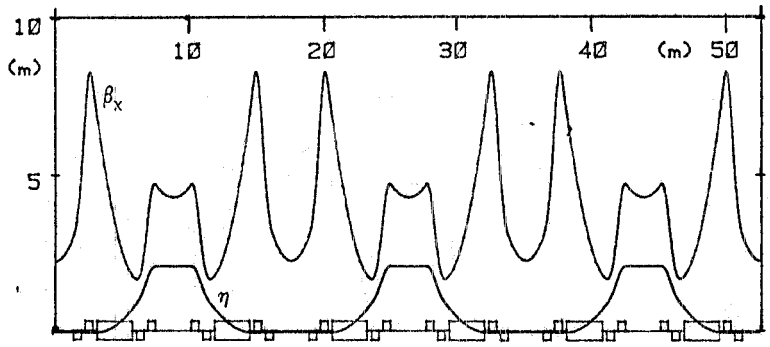

Fig. 10. Radial betatron function β_x and off-energy function η for half machine.

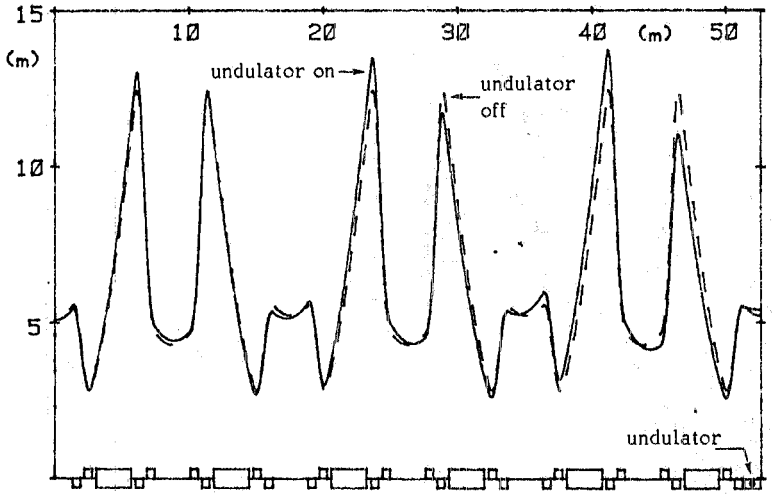

Fig. 11. Vertical betatron function β_z, with undulator on and off (in both cases ν_x = 5.15 and ν_z = 3.15), for half machine.

new optics are listed in Table II.

6. ELECTRON BUNCH LENGTHENING

As clearly shown in eq. (9), the FEL gain is seen to depend upon the electron peak current, or, equivalently, upon the RMS bunch length σ_y.

Table II - Parameters of the new Adone optics.

Electron energy	E = 610 MeV
Momentum compaction	$\alpha_c = 1.36 \times 10^{-2}$
Fractional energy spread	$\sigma_p = 2.3 \times 10^{-4}$
Invariant	$\langle H \rangle = 0.38$ m
Radial emittance (off coupling)	$A_x = 0.25$ mm x mrad
Energy loss in bending magnets	$U_o = 2.35$ keV/turn
Energy loss in undulator	$U_w = 109$ eV/pass
Radial and vertical betatron tunes	$\nu_x = 5.15$; $\nu_z = 3.15$
Radial and vertical natural chromaticities	$C_x = -1.06$ $C_z = -1.61$
Damping partition numbers and times	$J_s = 2$, $J_x = J_z = 1$; $\tau_i = 174/J_i$ msec
Revolution frequency	$f_o = 2.856$ MHz
RF frequency	$f_{RF} = 51.4$ MHz
Harmonic number	h = 18
Number of bunches	$n_b = 3$
RF peak voltage and acceptance	$V_{RF} = 300$ kV; $\varepsilon_{RF} = 3.58\%$

The anomalous bunch lengthening for the new Adone structure and RF cavity has been calculated following the phenomenological model of Chao-Gareyte[16] which proved to explain the old experimental data measured in Adone with the normal structure and the 8.56 MHz RF system[17].

The actual RMS bunch length can then be written as

$$\sigma_y\,(\text{cm}) \simeq 3.46\, i^{1/2.68}\ (\text{mA}) \qquad (11)$$

where i is the mean electron current per bunch

$$\left(i = I_p \frac{\sqrt{2\pi}\sigma_y f_o}{c}\right).$$

We just recall that the Chao-Gareyte model gives a bunch length independent from energy. Eq. (11) is plotted in Fig. 12 along with the natural (radiation) bunch length, vs. current.

Correspondingly, the maximum small signal gain per pass, as calculated for the LELA parameters, is plotted in Fig. 13 for the two cases of natural σ_y and anomalous lengthened bunch.

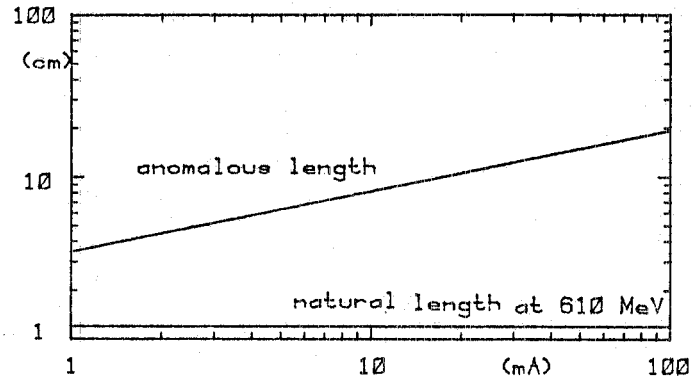

Fig. 12. Natural and anomalous bunch length σ_y for V_{RF} = 300 KV.

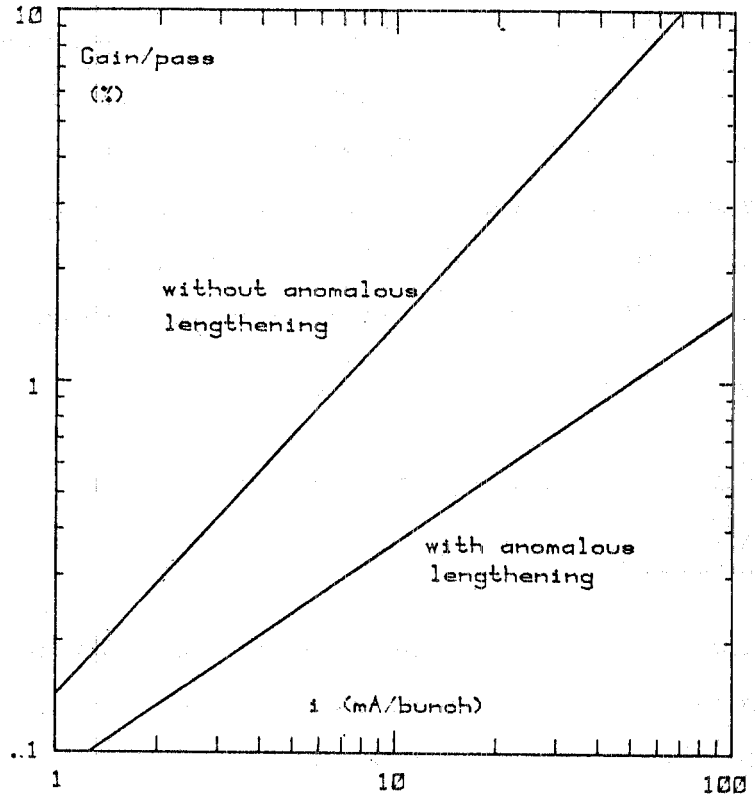

Fig. 13. Optical gain/pass vs. mean current/bunch.

We conclude that the anomalous lengthening significantly affects the gain. Accurate measurements at the energy and

currents considered, with the new RF system, will have to be performed. Our present thinking is that the Chao-Garey te type extrapolation gives an upper limit to the anomalous lengthening and, consequently, a lower limit to the gain. Further measurements on the beam are in progress[18].

7. THE EXPERIMENTAL PROGRAM

The planned experimental activity will consist essential ly in the measurement of first and third harmonic gain by using an external Argon Laser (CR 10), the construction and operation of an optical cavity (oscillator) and exploitation of the undulator in an optical klystron configuration.

7.1. First harmonic measurements

According to eq. (6) the FEL gain is inversely proportion al to the optical mode cross section $\langle \Sigma_L \rangle$ in the interaction region, provided the electron beam is fully contained within the laser beam ($\Sigma_e \lesssim \Sigma_L$).

The laser beam cross section $\langle \Sigma_L \rangle$ is given by

$$\langle \Sigma_L \rangle = \frac{1}{L_w} \int_{-L_w/2}^{L_w/2} \Sigma_L(y)\, dy = \tag{12}$$

$$= \frac{2\pi w_o^2}{L_w} \int_0^{L_w/2} \left[1 + \left(\frac{\lambda y}{\pi w_o^2} \right)^2 \right] dy$$

where L_w is the length of the interaction region and w_o is the beam waist for a TEM_{oo} gaussian mode. The optimum

beam waist can be found by minimizing the mode cross section

$$\frac{d}{dw_o} \langle \Sigma_L \rangle = 0 , \tag{13}$$

which implies

$$w_o = \sqrt{\frac{L_w \lambda}{2\pi\sqrt{3}}} . \tag{14}$$

By substituting eq. (14) into eq. (12) we have:

$$\langle \Sigma_L \rangle = \frac{L_w \lambda}{\sqrt{3}} . \tag{15}$$

For $\lambda = 5145$ Å (our experiment) the optimum beam waist becomes $w_o \simeq 0.35$ mm.

In Figs. 14a and 14b we show the e-beam and laser beam profiles along the interaction region in the radial and vertical plane, respectively.

The e-beam dimensions are plotted for two values of the betatron oscillation coupling factor $\chi^2 \simeq 0.4$ (circular e-beam) and $\chi^2 \simeq 0.01$, which corresponds to the minimum coupling experimentally obtained in Adone and gives an approximately flat beam.

The same laser beam waist will be produced both in the amplification and in the oscillator experiment. In the former case the external laser beam will be focussed by means of a lens transport system, while in the latter two mirrors will be added, at either end of the interaction region, to form an optical cavity 17.5 m long. Due to the existence of radia

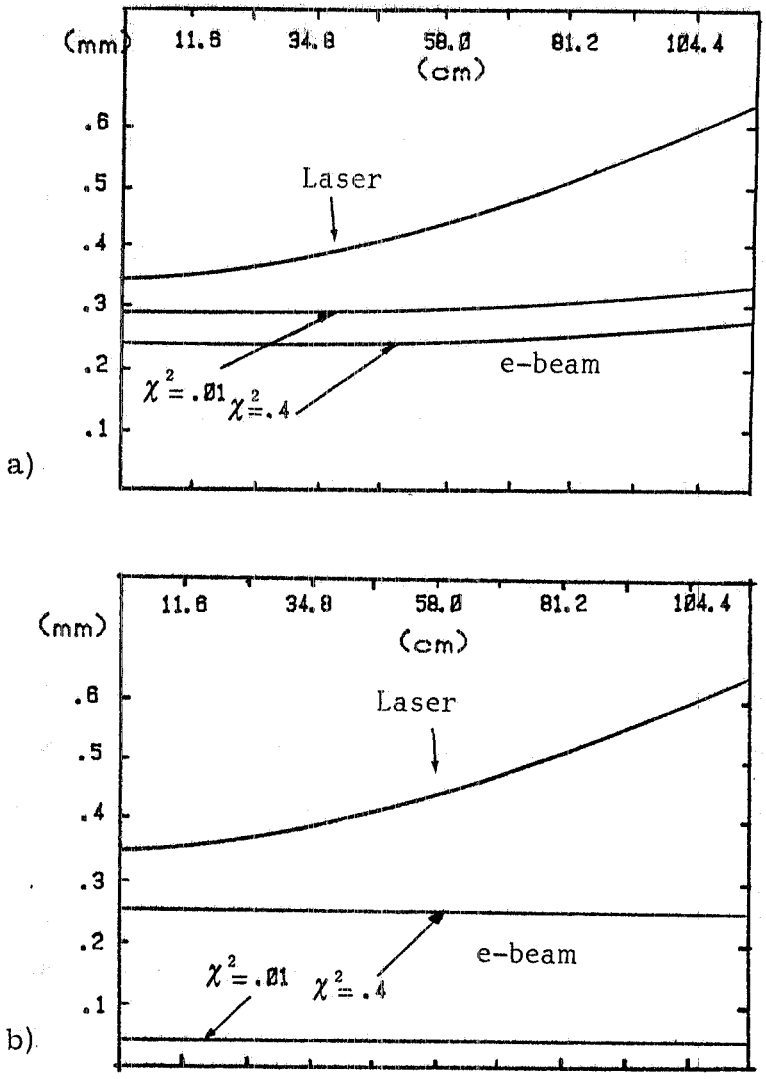

Fig. 14. Electron beam and laser beam profiles, along the interaction region. a) Radial plane; b) Vertical plane.

tion shielding walls, the mirrors will be placed asymmetrically with respect to the undulator mid-point and their curvature radii will be $R_1 \simeq 6.1$ m and $R_2 \simeq 11.5$ m, respectively. The gain measurement will be done by extracting the modulation at 2.85 MHz superimposed on the incoming la-

ser beam intensity by a lock-in technique very similar to that used in Madey's experiments[1,2,3].

Some work is also in progress for analysing the capability (and usefulness) of different techniques such as boxcar integration or fast Fourier transform methods.

7.2. Third harmonic measurement

Fig. 15a shows the spontaneous radiation spectrum (at zero degrees) folded with the e-beam angular and energy distributions ; Fig. 15b shows the gain profile as obtained by differentiating the spontaneous spectrum with respect to the electron energy[11].

By raising the undulator strength value to $K = 4$ and lowering the electron energy at $E = 410$ MeV, the external Argon laser may be made to interact with the spontaneous radiation third harmonic.

While the spontaneous radiation maximum is seen to decrease (Fig. 16a) the corresponding gain value increases by a factor $\simeq 2.7$ (Fig. 16b), which is mainly due to the spontaneous radiation line narrowing.

7.3. The optical klystron

In order to achieve an "optical klystron" configuration, the magnetic periodicity of the undulator must be changed so as to create a magnetic drift space in the middle of the structure. Two conditions must be fulfilled since the undulator is to be inserted in a storage ring:

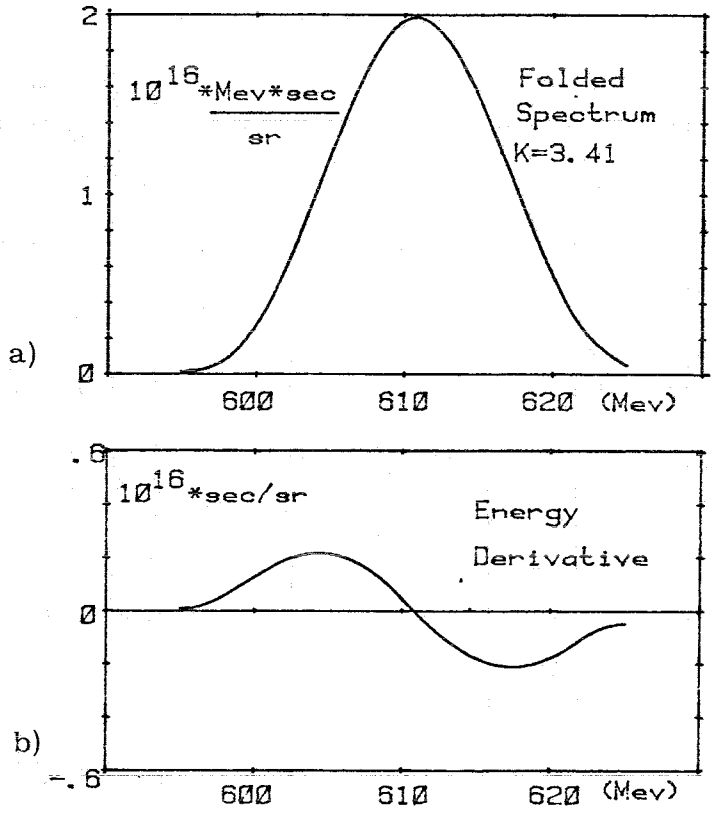

Fig. 15. a) First harmonic spontaneous spectrum; b) Derivative of the spontaneous spectrum.

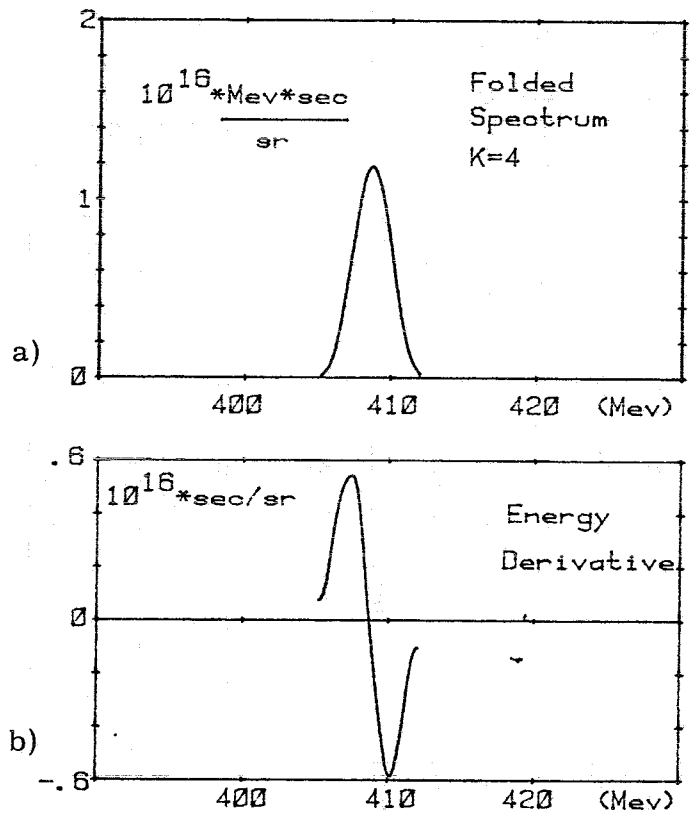

Fig. 16. a) Third harmonic spontaneous spectrum; b) Derivative of the spontaneous spectrum.

i) The field integral over the longitudinal coordinate must vanish: this ensures that no net deflection is acquired by an electron in traversing the structure.

ii) The second field integral (i.e. the integral over the radial electron velocity) must vanish as well, if no net displacement is to be suffered by the electron.

The shortest drift space fulfilling items i) and ii) is shown in Fig. 17a, and is obtained by reversing the polarity of the

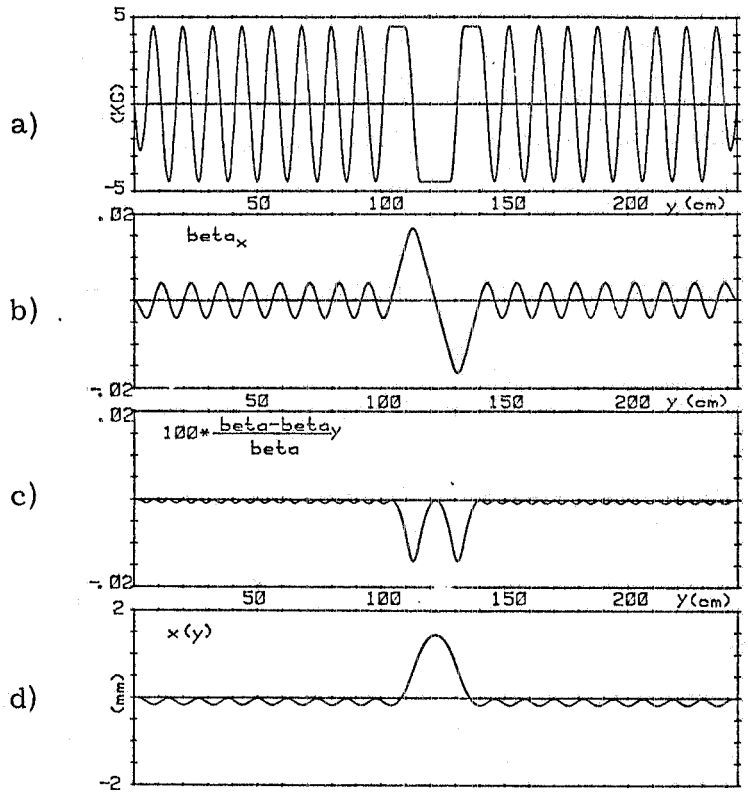

Fig. 17. Dynamics of the electron within an optical klystron modified undulator for E = 610 MeV and K = 3.41. a) Vertical field on axis; b) Transverse electron velocity (c units); c) Longitudinal electron velocity; d) Transverse displacement.

two pole pairs adjacent to the central pole, which simply implies to reverse the current flow in the corresponding coils.

The resulting drift space is 3 periods long and is sandwiched between two equal sections containing 16 inner poles plus one end pole each.

This sections are known in the literature as the "buncher" and the "radiator", respectively.

The actual vertical field distribution along the drift space after polarity inversion has been computed by the MAGNET code and is shown in expanded view in Fig. 18.

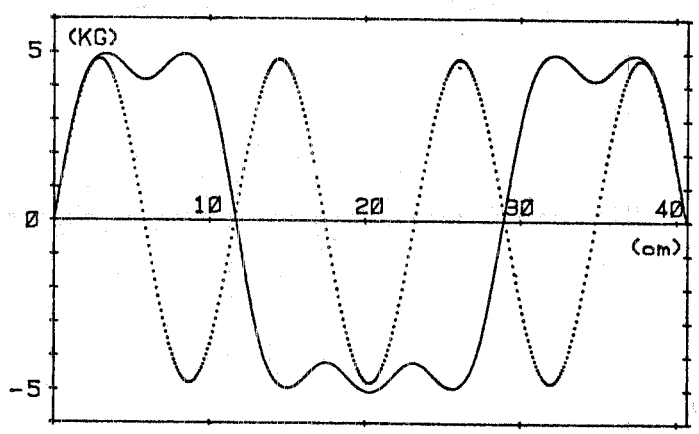

Fig. 18. Enlarged view of the modified magnetic field as computed by MAGNET. Dotted curve: normal configuration. Solid curve: magnetic drift space.

The electron radial and longitudinal velocity and the radial displacement are shown in Fig. 17b, c, d respectively. Due to the radial bump in the electron trajectory within the magnetic drift space, a time delay arises between radiation

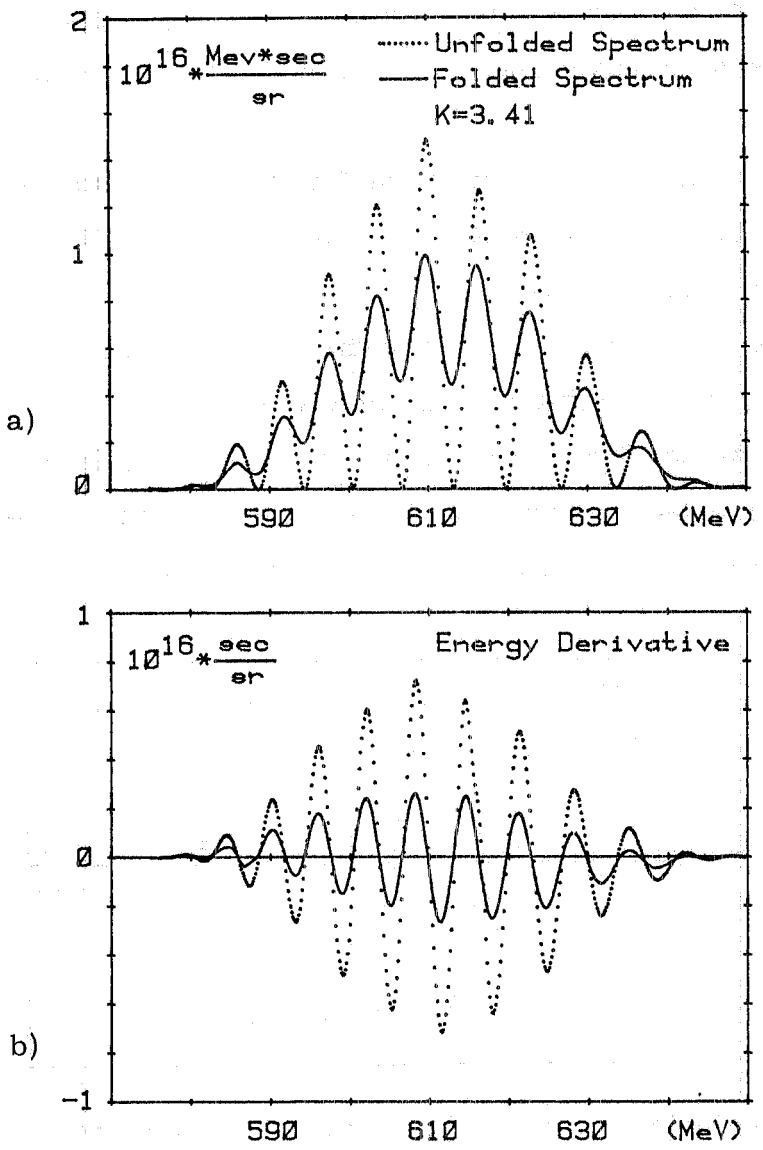

Fig. 19. a) Optical klystron spontaneous radiation spectrum at $\vartheta = 0$, $\lambda = 5145$ Å, vs. electron energy.
b) Energy derivative of the spontaneous spectrum.
Dotted curves: unfolded. Solid curves: folded up with e-beam energy and angular distributions.

wavetrains emitted in the buncher and in the radiator, which produces an interference-like effect[19] in the wavelength distribution of the overall radiation. The same happens to the distribution vs. electron energy (at a fixed wavelength), as shown in Fig. 19a, which was obtained by inserting the modified magnetic field pattern in the SINCLUCE radiation code.

By comparison between Fig. 19b (dotted curve) and Fig. 15b, we notice a gain enhancement of a factor ~ 3 as obtainable by the optical klystron configuration. However, if the e-beam energy and angular distributions are taken into account (Fig. 19b - solid curve) the result looks less favourable, since no apparent gain enhancement seems to be reached through the O.K. modification.

REFERENCES

1. L. R. Elias, W. M. Fairbank, J. M. J. Madey, H. A. Schwettman and T. I. Smith, Phys. Rev. Letters 36, 717 (1976).
2. D. A. G. Deacon, L. R. Elias, J. M. J. Madey, G. J. Ramian, H. A. Schwettman and T. I. Smith, Phys. Rev. Letters 38, 802 (1977).
3. D. A. G. Deacon, J. M. J. Madey, C. Bazin, M. Billardon, P. Elleaume, Y. Farge, J. M. Ortega, Y. Petrof, K. E. Robinson and M. F. Velghe, Proceedings of the 1981 Particle Accelerator Conference, Washington, March 1981.
4. R. Barbini and G. Vignola, LELA: A free electron laser experiment in Adone, Frascati report LNF-80/12 (1980).
5. D. D. Ivanenko and I. Ya. Pomeranchouk, DAN (URSS) 44, 343 (1944); D. D. Ivanenko and A. A. Sokolov, DAN (URSS) 59, 1551 (1948); J. Schwinger, Phys. Rev. 75, 1912 (1949); R. Chrien, A. Hoffmann and A. Molinari, Phys. Reports 64, 5 (1980).
6. D. Jackson, Classical Electrodynamics (Wiley, 1965).
7. R. Barbini and G. Vignola, SINCLUCE A computer ray-tracing code for evaluation of wiggler and undulator radiation, Adone int. Memo (unpublished).
8. J. M. J. Madey, private communication, and in "Free-Electron Generators of Coherent Radiation", Physics of Quantum Electronics, vol. 7, S. F. Jacobs et al. editors (Addison Wesley, 1979).
9. G. K. Green, Spectra and optics of synchrotron radiation, Brookhaven report BNL 50522 (1976).
10. Many authors derived the S. S. G. formula, with different approaches. See for instance: W. B. Colson, Phys. Letters 59A, 187 (1976); 64A, 190 (1977); F. A. Hopf, P. Meystre, M. O. Scully and W. H. Louisell, Optics Comm. 18, 413 (1976); Phys. Rev. Letters 37, 1342 (1976).
11. J. M. J. Madey, Nuovo Cimento 50B, 64 (1979).
12. Ch. Iselin, Program MAGNET - T600 : Method described

by R. Perin and S. Van der Meer, Report CERN 67-7 (1967).

13. R. Barbini, A. Cattoni, B. Dulach, C. Sanelli, M. Serio and G. Vignola, The LELA undulator, Frascati report LNF-80/62 ; to be published in Nucl. Instr. and Meth.

14. M. Sands, The physics of electron storage rings. An introduction, Report SLAC-121, UC-28(ACC) (1970).

15. M. Bassetti, A. Cattoni, A. Luccio, M. Preger and S. Tazzari, A transverse wiggler magnet for Adone, Frascati report LNF-77/26 (1977) ; M. Bassetti and S. Tazzari, in "Wiggler Meeting", Frascati, June 1978, ed. by A. Luccio, A. Reale and S. Stipcich (Laboratori Nazionali di Frascati, 1978).

16. A. W. Chao and J. Gareyte, Scaling law for bunch lengthening in SPEAR II, Report SPEAR 197/PEP 224 (1976).

17. S. Tazzari, Scaling dell'allungamento anomalo, Adone int. Memo T-93 (1978).

18. R. Boni, S. Guiducci, M. Serio, F. Tazzioli and F. Wang, Investigation on beam longitudinal transfer function and coupling impedance in Adone, Adone int. Memo RM-23 (1981).

19. A. S. Artamonov, B. A. Vinokurov, P. D. Voblyi, E. S. Gluskin, G. A. Kronyukhin, V. A. Kochubei, G. N. Kulipanov, V. N. Litvnenko, N. A. Mezentsev and A. N. Skrinsky, Nucl. Instr. and Meth. 177, 247 (1980).